J. Astron. Space Sci. 22(3), 197–210 (2005)

TWO-COLOR VR CCD PHOTOMETRY OF THE INTERMEDIATE POLAR 1RXS J062518.2+733433

Yonggi Kim[1,2†], Ivan L. Andronov[3,4,1], Sung Su Park[1], Lidia L. Chinarova[3], Alexey V. Baklanov[3], and Young-Beom Jeon[5]

[1]University Observatory, Chungbuk National University, Cheongju 361-763, Korea
[2]Institute for Basic Science Research, Chungbuk National University, Cheongju 361-763, Korea
[3]Department of Astronomy and Astronomical Observatory, Odessa National University, T. G. Shevchenko park, UA 65014, Odessa, Ukraine
[4]Crimean Astrophysical Observatory, UA 98409 Nauchny, Ukraine
[5]Korea Astronomy and Space Science Institute, Daejeon 305-348, Korea
email: ykkim153@chungbuk.ac.kr, ilandronov@onu.edu.ua, uavso@pochta.ru

(Received May 18, 2005; Accepted August 9, 2005)

ABSTRACT

Results of 7 nights of CCD VR photometry of the intermediate polar 1RXS J062518.2 +733433 obtained at the Korean 1.8m telescope are reported. The corrected ephemeris for the orbital minimum is BJD (Orb.min) = 2453023.6159 (42)+0.1966431 (33) (E-1735). The corrected ephemeris for the spin maximum is BJD (spin max) = 2452893 .78477 (10)+0.01374116815 (17) (E-15382) (cycle numbering corresponds to that of Staude et al. 2003). The variations of the shape of the individual spin variations are highly correlated in V and R. The phase of the *spin* maximum is found to be dependent on the *orbital* phase. The corresponding semi-amplitude of sinusoidal variations of phase is 0.11 ± 0.03. This new phenomenon is explained by the changing viewing conditions of the accreting magnetic white dwarf, and should be checked in further observations this star and for other intermediate polars. To avoid influence of this effect on the analysis of the long-term spin period variations, the runs of at least one orbital period are recommended. Results of time series analysis are presented in tables.

Keywords: cataclysmic variables, intermediate polars, RXS J062518.2+733433, BG CMi, FO Aqr.

1. INTRODUCTION

The X-Ray source 1RXS J062518.2+733433 (hereafter RXJ0625) has been classified as a cataclysmic variable (CV) by Wei et al. (1999). It has to be found to be an intermediate polar (IP) by Araujo-Betancor et al. (2003) and Staude et al. (2003). Such systems consist of a red dwarf filling its Roche lobe, and a magnetic white dwarf, which rotates (spins) much faster than the orbital motion. Two bright accretion columns with changing orientation cause two humps at the light curve, the relative height of which is dependent on the difference of viewing conditions for both poles. The IPs generally exhibit variations of the spin period P_{spin} (see e.g. Warner 1986, 1995, Patterson 1994, Hellier 2001 for reviews).

†corresponding author

Moreover, even the spin period itself needs more correct determination, as its original accuracy estimate leads to a huge uncertainty of 5.8 cycles per year (Araujo-Betancor et al. 2003). Staude et al. (2003) have improved the value of the spin period, so this error has significantly decreased to 0.1 cycles per year. However, for studies of the rotational evolution of magnetic white dwarfs in IPs, a long time-base monitoring is needed. So we have included the object in the list of key targets of the $Inter - Longitude\ Astronomy$ project (Andronov et al. 2003). Recently, we have detected a deceleration of acceleration ($\ddot{P}_{spin} > 0$) in BG CMi (Kim et al. 2005a) and, alternatively, "acceleration of acceleration" ($\ddot{P}_{spin} < 0$) in FO Aqr (Andronov et al. 2005c).

In this Paper, we present results based on 6 nights of VR CCD-photometry obtained in 2004-2005 at the Korean 1.8 m telescope and on one night obtained at the 60-cm telescope of the Korea Astronomy and Space Science Institute.

2. COMPARISON STARS

The observations have been obtained with a thinned SITe 2k CCD camera attached to the 1.8m telescope of the Bohuynsan observatory (Korea). The instrumental V and R systems have been used. An integration time was 30s. To determine instrumental magnitudes of stars, the IRAF/DAOPHOT package (Massey & Davis 1992) has been used. For the final determination of magnitudes, the computer program MCV (Multi-Column View) by Andronov & Baklanov (2004) have been used, which realizes the method of multiple comparison stars (see Kim et al. 2004).

The finding chart is shown in Figure 1. For the 1.8m telescope with a smaller field of view, only the relatively bright objects C1-C7 have been measured as the candidates to the comparison stars. Brighter stars show smaller scatter, it is effective to measure few bright stars in the field, as fainter stars have lower weight and their contribution to the improvement of accuracy of the "mean weighted" (or "artificial" comparison star) is negligible. For the 1.8m telescope, only seven "valuable" comparison stars are visible at the images, and they have been measured. For the 60-cm telescope, the field of view is larger, and another star has been added as a candidate to the comparison stars. However, this star GSC 04370-00206 had shown an obvious high-amplitude variability, as one may see in Figure 3.

This discovery of a new variable has been briefly reported by Kim et al. (2005c). The light curve of this new variable is typical for the EW type WUMa stars (Kim et al. 2005b). The range of R brightness variations is $13.^{m}05$-$13.^{m}46$ with a preliminary period estimate of $P = 0.^{d}4421 \pm 0.^{d}0018$. The minimum time $T_0 = 2453062.17715 \pm 0.^{d}00011$ had been obtained using the asymptotic parabola fit (Marsakova & Andronov 1996). The accuracy estimate of a single point for this star, as determined from the $\sigma-$scalegram analysis (Andronov 1997), is $0.^{m}005$. For further CCD observations of RXJ0625, it should be recommended to observe GSC 04370-00206 simultaneously in the same field of RXJ0625, if possible.

The brightness of the comparison star C2 has been determined by K.A.Antoniuk by linking to the UBVRI standard Gliese 277.1 (Gliese & Fahress 1979) with coordinates $\alpha_{2000} = 07^h34^m27.4^s$, $\delta_{2000} = +62°56'29"$ and is equal to $U = 15.^{m}038(65)$, $B = 14.^{m}381(21)$, $V = 13.^{m}461(23)$, $R = 12.^{m}732(10)$, $I = 12.^{m}201(11)$ (Andronov et al. 2005a). These values are slightly different with that used by Araujo-Betancor et al. (2003) ($V = 13.^{m}4 \pm 0.^{m}4$) and Staude et al. (2003) ($R = 12.^{m}89$), but are in a good agreement with the photometry ($V = 13.^{m}482(6)$) by Henden (2004a).

Unfortunately, no R photometry of the comparison stars had been published yet. Thus we had made an indepentent brightness estimate based on two-color BV photometry by Henden (2004a) and the statistical $color - color$ relations. For this purpose, we have used BVR photometry of the stars

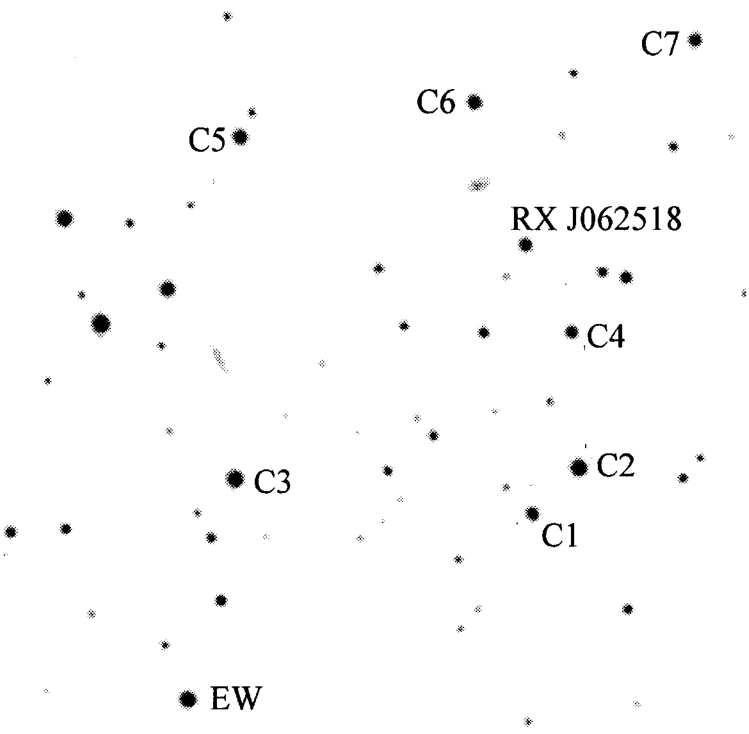

Figure 1. Finding chart for RXJ0625 and a newly discovered EW-type variable GSC 04370-00206. The field is $6' \times 4.8'$, North is up and East is left.

in the field of V1315 Aql by Henden (2004b) to have the same *standard* photometric system. The stars at the "$(V-R)-(B-V)$" diagram lie at some sequence, which is shown in Figure 2. The sample has been shortened to the stars with $V < 18.^{\rm m}0$, $B < 20.^{\rm m}2$, altogether 75 objects. The most left point is an outstanding one, despite it corresponds to a relatively bright star with $V = 14.^{\rm m}495$. However, the error estimate is rather large ($\sigma_{B-V} = 0.^{\rm m}247$), so the star was not used for further analysis. One may suspect that it may be a variable star, but that field is not studied in the present paper.

In the range of $(B-V)_H$ from $0.^{\rm m}2$-$1.^{\rm m}454$, the dependence for 25 stars is nearly linear:

$$(V-R)_H = -0.^{\rm m}013(23) + 0.6075(202)\cdot(B-V)_H \quad (1)$$

with a r.m.s. deviation of individual points from the fit of $0.^{\rm m}026$. Here the index "H" corresponds to the magnitudes derived by Henden (2004b). For larger values of $(B-V)_H$, the dependence becomes non-linear and much more scattered, but this range is not covered by our comparison stars, so we may use this statistical dependence in a linear form.

Using Eq. (1), we have computed the extrapolated values of brightness $R_H = V_H - (V-R)_H$, which are listed in Table 1 for comparison with the *instrumental* magnitudes (indexed by "i") obtained using the UBVRI brightness of the star C2 and the mean instrumental magnitude

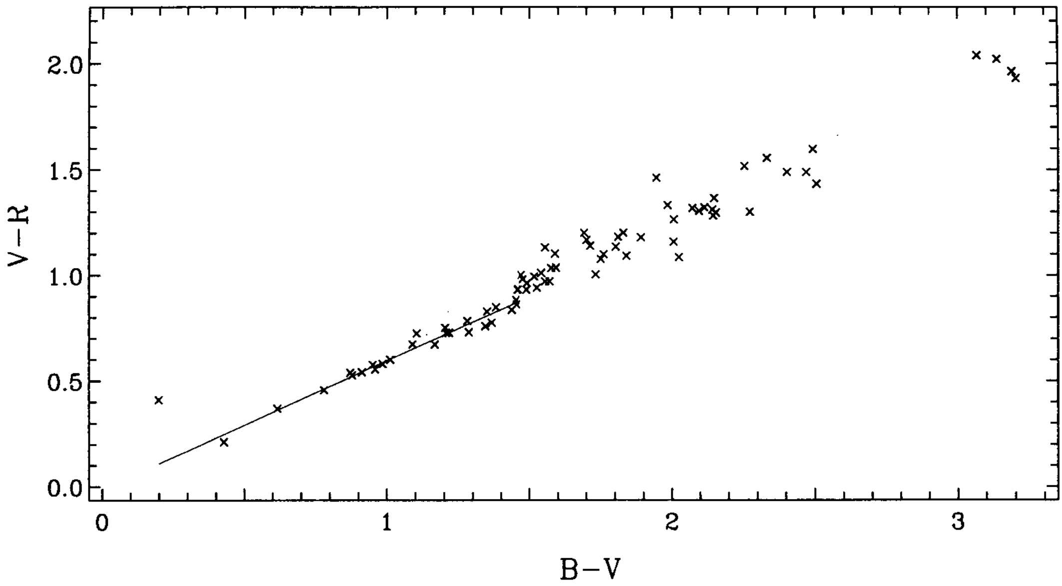

Figure 2. The "color-color" diagram for 75 stars in the field of V1325 Aql according to the data by Henden (2004b) with $V < 18.^{m}0, B < 20.^{m}2$ (crosses). The left point is an outstanding one and was removed for further analysis. The line corresponds to the linear fit from Eq. 1 for the range $B - V < 1.454$.

differences for 4 best nights. For comparison, we use only the stars C1-C7, as EW marks a newly discovered EW-type variable star. The *Henden* V magnitudes are systematically larger by $0.^{m}035$ (12) than the *instrumental* ones.This shift is much larger for $0.^{m}204$-$0.^{m}289$ with a mean value of $0.^{m}263$ (28). This means that the color index shift is $(V-R)_H-(V-R)_i = -0.^{m}228(24)$ (-$0.^{m}183$ for the *main* comparison star C2).

Such large systematic difference is owed to the difference between the *standard* R systems of Henden (2004b) and Gliese & Fahress (1979), which are based on CCD and photoelectric photometry, respectively. As usually, the difference in V is much smaller, than in other colors. The "$(V-R)_H - (V-R)_i$" diagram shows just the shift, the slope is unity within statistical errors. This means that the mean values of the color index may be shifted in respect to any other photometric system. However, this should not affect the amplitude and shape of variability of brightness and color index. Thus we will continue to use the *instrumental* system, as the values R_H have been obtained using a non-direct procedure.

The unbiased estimates of the r.m.s. deviations of the individual magnitudes from the mean, σ_V and σ_R for two colors (see Kim et al. 2004 for details), which have been computed for 4 nights obtained at 1.8m in 2004, are listed in Table 1. The largest scatter is seen for the stars C1 and C3 both in V and R, so it may be recommended to exclude these stars from the list of comparison stars. There is a possible variability event for C7, which had been observed in 2005, and had not affected the data for 2004. However, we have excluded this star as well, and will check it's variability during further observations.

These values for the stars of the brightness similar to that of the variable (RXJ0625) are $\sim$ $0.^{m}007$ for both V and R, whereas the r.m.s. amplitudes of the intrinsic variability exceed this value

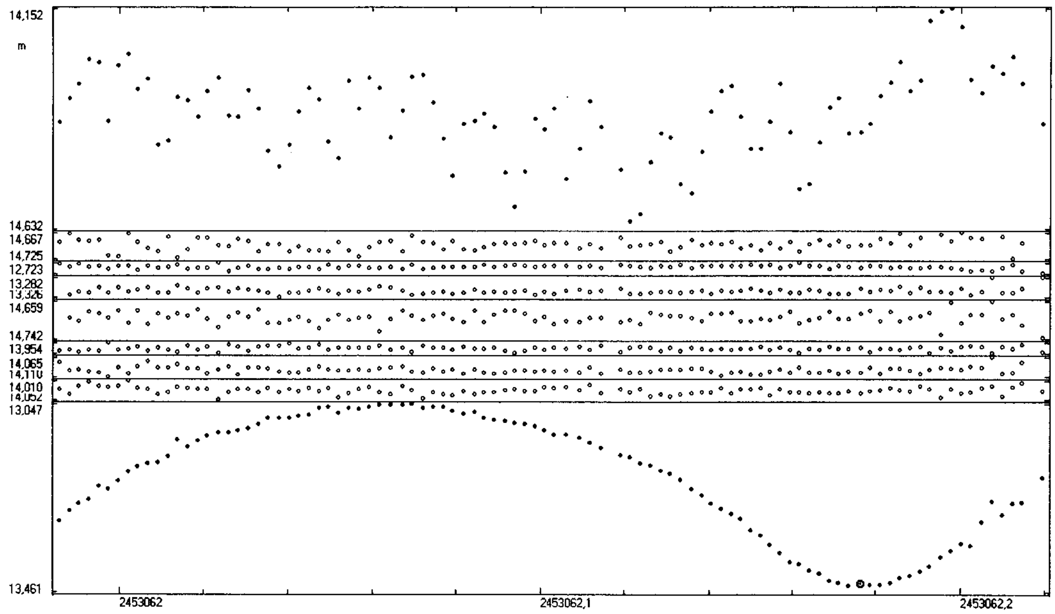

Figure 3. Brightness estimates of RXJ0625 (up), comparison stars C1-C7 and a newly discovered EW-type variable (bottom) using the method of Multiple comparison stars. The figure is a screenshot saved from the program MCV for Windows (Andronov & Baklanov 2004) for the night obtained at the 60-cm telescope in the filter R. The magnitude scale is the same for all stars. One may clearly see orbital+spin variations of RXJ0625 and the EW-type variability of one of candidates to the comparison stars.

by a factor of > 18. Thus the signal/noise ratio is large enough to make further analysis of the light curve.

3. JOURNAL OF OBSERVATIONS AND EFFECTIVE RUN CHARACTERISTICS

The journal of observations is presented in Table 2. All together 7 nights of observations from February 2004 to February 2005 have been obtained with a total duration of 30.6 hours (92.8 spin periods). Six nights were obtained at the 1.8m telescope with alternatively changing VR filters, and one night at the 60 cm telescope. For that run, the integration time had been increased, so no filter change was done because of a short spin period of $\approx$ 20 minutes. As the runs in V and R are mostly overlapping, the formal total duration in V and R is 55.6 hours (169 spin periods).

As a characteristic of the observed variability (consisting of the intrinsic variability of the system and of the observational noise), we have used two parameters - the r.m.s. deviation σ of data points from the sample mean and the peak-to-peak amplitude Δm. Despite both characteristics are dependent on few parameters, e.g. distribution of observations in phases of orbital and spin periods, atmospheric transparency and stability etc., there is a good correlation between them, which may lead to an approximate statistical relation $\Delta m = \zeta\sigma$ with $\zeta = 5.01(18)$ (unweighted approximation) and $\zeta = 4.57(16)$ (weights inverse proportional to σ^2). These values coincide within their error estimates.

Table 1. Brightness and colors of the stars in the field of RXJ0625 in the *instrumental*("i") system and in the *standard*system (Henden 2004a). The R_H are R magnitudes extrapolated from the V_H and $(B-V)_H$ values using the Eq. 1.

N	Name	V_H	$(B-V)_H$	R_H	V_i	σ_V	R_i	σ_R	$(V-R)_i$
C1	N2101313460 (gsc2.2)	15.331	0.661	14.942	15.292	0.0123	14.654	0.0134	0.638
C2	GSC 04370-00234	13.482	0.920	12.936	13.461	0.0055	12.732	0.0081	0.729
C3	GSC 04370-00210	13.956	0.681	13.555	13.920	0.0117	13.289	0.0122	0.631
C4	N2101313553 (gsc2.2)	15.292	0.592	14.945	15.256	0.0102	14.673	0.0068	0.582
C5	GSC 04370-01007	14.610	0.651	14.228	14.559	0.0080	13.951	0.0077	0.608
C6	GSC 04370-00988	14.770	0.739	14.334	14.723	0.0069	14.075	0.0075	0.649
C7	GSC 04370-01048	14.984	1.172	14.285	14.966	0.0087	14.009	0.0069	0.957
EW	GSC 04370-00206	13.985	0.761	13.536					

Table 2. Journal of observations: the designation of the run (integer part of HJD-2453000 and the filter) HJD of the start t_s and end t_e of the run, the number of data points n, the sample mean $\bar{m}$ and the r.m.s. deviation σ of data points from the sample mean, the minimal m_{min} and m_{max} maximal magnitude, the peak-to-peak amplitude Δm, the time resolution δt in seconds and the duration of the run D in hours.

Run	$t_s-2453000$	$t_e-2453000$	n	$\bar{m}$	σ	m_{min}	m_{max}	Δm	δt	D
049 V	049.1710	049.2437	29	14.788	0.074	14.666	14.954	0.287	112	1.8
049 R	049.1689	049.2448	30	14.380	0.070	14.268	14.541	0.273	113	1.9
050 V	050.9323	051.3289	228	14.806	0.126	14.477	15.102	0.625	75	9.6
050 R	050.9336	051.3297	228	14.383	0.116	14.090	14.659	0.569	75	9.5
053 V	053.1385	053.2566	73	14.699	0.093	14.473	14.884	0.411	71	2.9
053 R	053.1393	053.2573	73	14.269	0.087	14.072	14.449	0.378	71	2.9
054 V	054.1369	054.2024	38	14.680	0.084	14.511	14.871	0.360	76	1.6
054 R	054.1376	054.2031	38	14.244	0.082	14.082	14.405	0.322	76	1.6
061 R	061.9856	062.2146	95	14.374	0.096	14.136	14.612	0.476	105	5.6
384 V	384.1826	384.3977	92	15.689	0.156	15.312	16.057	0.745	102	5.2
384 R	384.1836	384.3988	91	15.148	0.154	14.758	15.429	0.671	103	5.2
405 V	405.9714	406.1317	50	15.740	0.225	15.152	16.478	1.326	141	3.9
405 R	405.9738	406.1331	49	15.234	0.204	14.773	15.857	1.083	143	3.9

4. LONG-TERM BRIGHTNESS AND COLOR VARIATIONS

The night-to-night variability of the mean brightness $\bar{m}$ is present. However, the seasons 2004 and 2005 show a clear difference in the activity state. In 2004, the star was much brighter ($\bar{V} = 14.^{m}770(6)$, $\bar{R} = 14.^{m}346(6)$) than in 2005 ($\bar{V} = 15.^{m}707(15), \bar{R} = 15.^{m}178(15)$). The corresponding differences of seasonal mean magnitudes are $(\bar{V}_{2005} - \bar{V}_{2004}) = 0.^{m}937(16)$ and $(\bar{R}_{2005} - \bar{R}_{2004}) = 0.^{m}832(16)$, so the amplitude decreases with wavelength in the observed spectral range. This causes an increase of the color index from $(V-R)_{2004} = 0.^{m}424(9)$ to $(V-R)_{2005} = 0.^{m}529(21)$.

A preliminary interpretation of this *reddening* (i.e. a larger value of the color index $V-R$ in the low luminosity state than in the high state) of the object in a state of low brightness is the decrease of the mass transfer rate and thus of the high-temperature emission, thus the relative contribution from the red dwarf increases. However, for a firm conclusion, a detailed study of spectral energy distribution in both high and low luminosity states is needed. From the present work, we may only justify the difference of color indices and thus the reddening in the low state.

In both seasons, the night-to night variability of the sample mean is within $0.^{m}05$-$0.^{m}15$ similar to that observed in other intermediate polars (cf. Patterson 1994, Andronov et al. 2005b,c).

5. CORRECTION OF THE SPIN PERIOD

The most precise published ephemeris

$$\mathrm{BJD}_{max} = 2452682.4181(5) + 0.^{\mathrm{d}}01374127(5) \cdot E \tag{2}$$

had been obtained by Staude et al. (2003) using a compilation of their own maxima timings and that obtained from the photometric data of Araujo-Betancor et al. (2003). For the further O-C analysis, we have applied a 3-period fit similar to that used by Kim et al. (2005a) for another intermediate polar BG CMi:

$$\begin{aligned} m(t) &= C_1 + C_2\cos(\omega_o t) + C_3\sin(\omega_o t) + C_4\cos(2\omega_o t) + C_4\sin(\omega_o t) \\ &\quad + C_6\cos(\omega_s t) + C_7\sin(\omega_s t), \end{aligned} \tag{3}$$

where $\omega_o = 2\pi/P_o$, $\omega_s = 2\pi/P_s$, and P_o and P_s are orbital and spin periods, respectively. As initial values, we have used $P_o = 0.^{\mathrm{d}}19661$ and $P_s = 0.^{\mathrm{d}}01374127$ by Staude et al. (2003). During a one-night run, the difference of the fits obtained using these and *true* (possibly slightly other) values is negligible, as one may justify from the results obtained below.

The nightly characteristics of the sinusoidal spin contribution are listed in Table 3. Besides the *nightly* moment of maximum, which is closest to the sample mean time of observations (see Andronov (1994) for details), the semi-amplitude $r = (C_6^2 + C_7^2)^{1/2}$ is listed, as well as the cycle number and phase according to the ephemeris (Eq. 2). The corresponding O-C diagram is shown in Figure 4. It shows a statistically significant (20σ) negative trend. Thus an improved ephemeris for 29 maxima timings (16 published by Staude et al. (2003) and 13 from the Table 3 of the present work) is

$$\begin{aligned} \mathrm{BJD}_{max} &= 2452682.41812(13) + 0.^{\mathrm{d}}01374116815(17) \cdot E \\ &= 2452893.78477(10) + 0.^{\mathrm{d}}01374116815(17) \cdot (E - 15382). \end{aligned} \tag{4}$$

Here we have used the equal weights, as the accuracy estimates for the previously published timings are not known. The period in Eq. 4 is much more accurate, as it spans much larger time interval. We have checked for the possible period variations $\dot{P}$, which are usually seen in intermediate polars. The parabolic fit does not deviate significantly from the line. However, the cubic parabola seems to be statistically significant with an ephemeris

$$\mathrm{BJD}_{max} = 2452682.41810(24) + 0.013741329(61)E - 7.1(2.7)10^{-12}E^2 + 7.8(3.0)10^{-17}E^3. \tag{5}$$

The deviation of the last coefficient from zero is 2.6σ, which corresponds to the false alarm probability (FAP) of 0.0093. Such an ephemeris fits well both the early observations compiled by Staude et al. (2003), which have a zero slope, and our data for 2004 and 2005 with a slope significantly deviating from zero by 19.7σ. However, the suggestion on the period variation should be checked either by possible unpublished data between the groups of points and by further monitoring of this interesting object.

6. ORBITAL PERIOD

Staude et al. (2003) have published an ephemeris

$$BJD(orb) = 2452682.463(3) + 0.^{\mathrm{d}}19661(27) \cdot E, \tag{6}$$

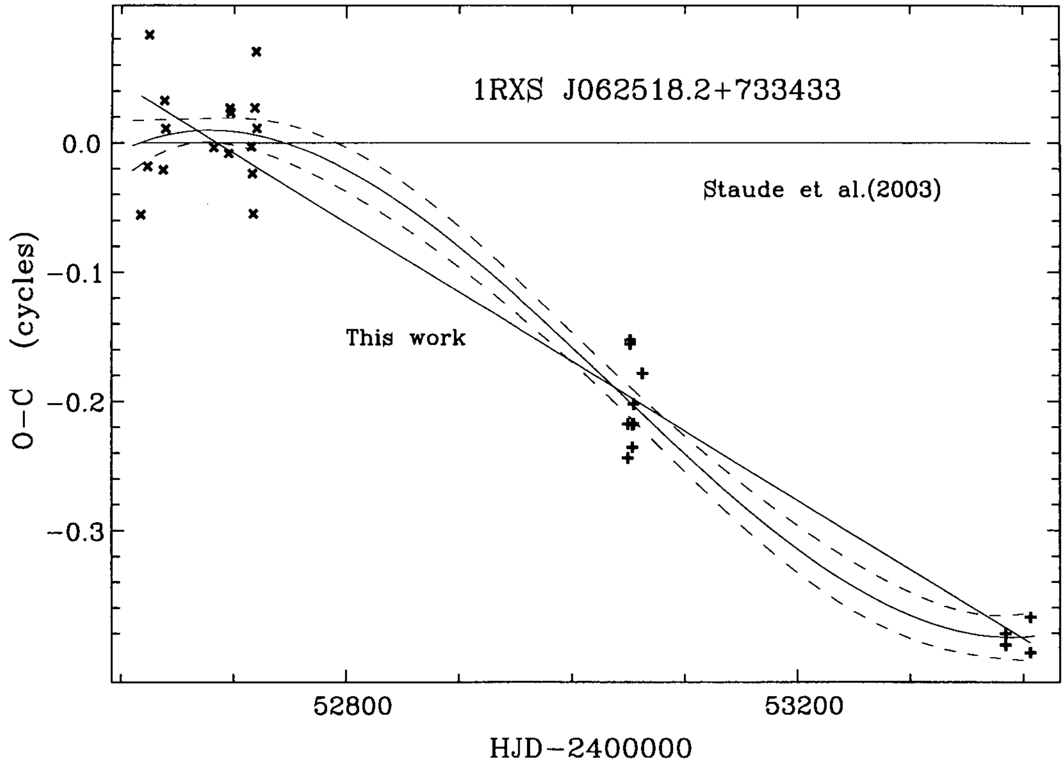

Figure 4. O-C diagram for the spin maxima according to the ephemeris (Eq. 4). The data published by Staude et al. (2003) are marked as $\times$, our maxima are marked as $+$. The straight lines correspond to the ephemeris by Staude et al. (2003) and that obtained in the present work (Eq. 4). The curved line and dashed lines show the cubic ephemeris (Eq. 5) and the corresponding "1σ" error corridor.

with a period of P_o and an initial epoch T_0 (corresponding to the sharp rise from minimum) contrary to the usual minima timings. Because of a relatively short time interval of their observations of 38^d, the error estimate of the frequency is large and reaches $2.5P_o/\mathrm{yr}$. Thus the orbital period also needs a correction.

In an addition to their individual timings, we had determined the mean phases and timings using their published Figure 5. This graph had been digitized by using 300 dpi resolution, i.e. 390 pixels per orbital period. For each pixel column, the black-colored pixel was treated as an observation, and a corresponding mean and r.m.s. deviations have been computed. For an error estimate of the mean, we have used a typical diameter of each point of 4 pixels. Of course, many points are overlapping, but it is not possible to take this into account. A mean accuracy estimate for such a point is $\sim 0\overset{m}{.}01$, a reasonably small value for a further analysis.

The corresponding *runningmean* curve shows a nearly flat minimum from the phase 0.765 to 1. The middle of this minimum corresponds to a phase 0.883. No prominent dip after the mid-minimum, likewise in another intermediate polar BG CMi (Kim et al. 2005a) is observed. To avoid possible systematical errors, we have used the same two-harmonic fit for this light curve, similar to the 3-period fit for our individual light curves. The corresponding phase of the minimum 0.894

Table 3. The times of minima determined using two-harmonic approximation of the orbital variability. The phases are computed according to the ephemeris by Staude et al. (2003).

$t_{min} - 2453000$		ϕ_{min}	$t_{min} - 2453000$		ϕ_{min}	$t_{min} - 2453000$		ϕ_{min}
Orbital minima								
53050.9494	R	0.195	53051.1456	V	0.193	53384.2879	V	0.625
53050.9490	V	0.195	53062.1276	R	0.049	53406.0674	R	0.400
53051.1460	R	0.195	53384.2836	R	0.603	53406.0617	V	0.371
Artificial orbital minima obtained from maxima (shifting by $-0.^d0679$).								
53049.1569	V	0.077565	53054.0896	V	0.166319	53062.1279	R	0.050811
53049.1613	R	0.099944	53054.0903	R	0.169879	53384.2828	V	0.598698
53053.1528	R	0.401556	53061.9313	R	0.050862	53384.2830	R	0.599715

(or –0.106) is only by 0.01P shifted in respect to an asymmetric mid-minimum, so both methods had given consistent results. The last phase estimate had been used to determine an artificial timing corresponding to the median of the interval covered by the observations by Staude et al. (2003): $T_{min} = 52701.5143(E = 97)$.

This mean time had been added to 7 timings published by Staude et al. (2003). For our observations, the minima timings have been determined by using a two-harmonic part of the three-period fits. They are listed in the Table 3. For some nights, both minima and maxima had been observed. The time difference between them is within $0.^d005$ equal to that $0.^d0679=0.345P_o$ obtained from the mean phase curve of Staude et al. (2003). So we have determined 9 *artificial* minima by shifting the maxima by this constant value. They are also listed in Table 3.

Assuming the cycle counting is corresponding to the ephemeris by Staude et al. (2003), the following ephemeris had been determined using their 8 timings, as well as 9 timings of the observed minima and 9 observed maxima:

$$\begin{aligned} BJD_{Orb.Min} &= 2452682.4400(71) + 0.1966431(33) \cdot E \\ &= 2453023.6159(42) + 0.1966431(33) \cdot (E - 1735). \end{aligned} \quad (7)$$

This ephemeris correction had been obtained using the OL software (Andronov 2001). The statistical frequency error of $0.03P_o$/year is much smaller than previously published one. Despite the minima in V and R are very close in time, the phase shifts of these pairs from this ephemeris are very large - from -0.15 to +0.20. The r.m.s. scatter of phases is relatively large: $0.107P_o$. This may be an argument against the hypothesis of the grazing eclipse of the accretion disk by the red dwarf secondary, as e.g. in the case of BG CMi (Hellier 2001).

To check the possible period miscount, we have computed a periodogram for these 26 timings using the PERMIN software (Andronov 1991). The best fit ephemeris is the following:

$$BJD_{Orb.Min} = 2453023.6461(35) + 0.1964198(27) \cdot (E - 1737) \quad (8)$$

with a slightly smaller r.m.s. scatter of phases of $0.087P_o$. This ephemeris corresponds to the cycle number of the last timing $E_{26} = 3684$, whereas for the period of Staude et al. (2003), $E_{26} = 3680$. So the difference between the corresponding frequencies is 2 cycles/year. The period of Araujo-Betancor et al. (2003) is intermediate between these two estimates, thus differing by 1 cycle/year. So the yearly biases do not allow to determine a true cycle numbering. Thus one may recommend to make the future monitoring of this object at various seasons of the year.

As an independent checking of the ephemeris, we have used the mean light curve folded over the orbital phase (Figure 8 of Araujo-Betancor et al. 2003). The curve has been digitized and also

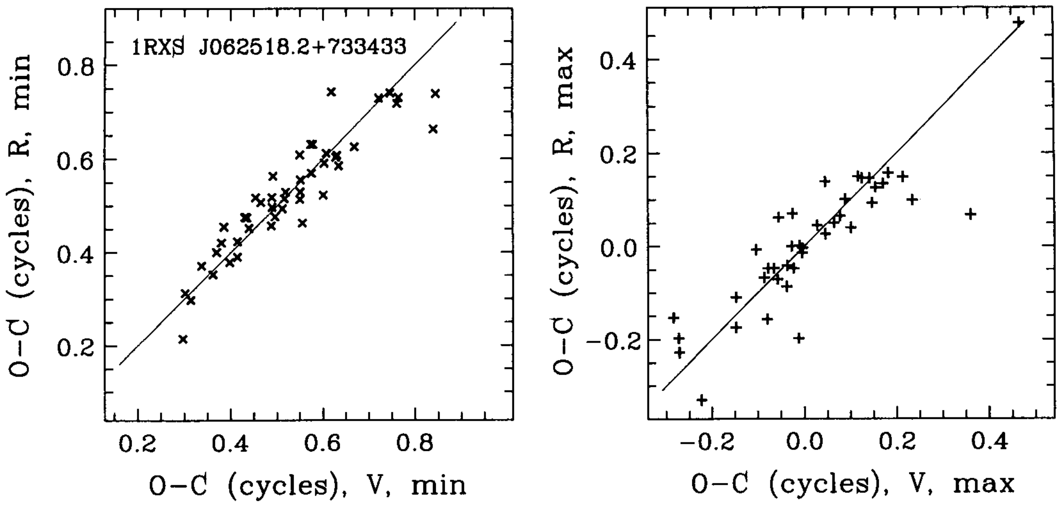

Figure 5. The phases of maxima and minima for V and R observations of individual spin pulses. The straight lines correspond to the equal phases.

fitted by a two-harmonic fit. The minimum of the fit occurs at the phase 0.859, thus corresponding to an additional timing of minimum at BJD 2452617.6768. However, this point stands at the opposite phase at the O-C diagrams for both our ephemeris and that of Staude et al. (2003). The examination of Figure 2 in Araujo-Betancor et al. (2003) shows that this time corresponds to a prolonged maximum (averaging the spin variability), and the minimum at this night occurs at JD 2452617.58, i.e. by $0.49P_o$ earlier! This minimum, as well as another one observed at JD 2452638.58, are in a good agreement with our ephemeris (Eq. 7), contrary to the alternate ephemeris (Eq. 8).

Having no original data, we can't make a detailed analysis of the origin of this contradiction. We may just suggest that this is a phenomenon of statistical fluctuations, when a *mean – subtracted* magnitude had been determined over a short observational run not covering the complete phase interval. Maybe such a bias had caused an exchange of phases of minimum and maximum. Using these periods, we can estimate the phase difference between the time of blue-to red crossing of the narrow component of He I λ 6678 (which is usually interpreted by irradiation of the secondary star) T_{He} = 2452617.508(5) (Araujo-Betancor et al. 2003) and the mean timing of the mid-eclipse T_{min} = 52701.5143 obtained in this work using the graph by Staude et al. (2003): $(T_{min} - T_{He})/P_o$ = 427.20 and 427.69 for the ephemerids (Eq. 7) and (Eq. 8), respectively. This difference is large for correct phasing of the spectral initial epoch.

7. INDIVIDUAL MINIMA AND MAXIMA OF THE SPIN VARIABILITY

Following Andronov et al. (2005a), we have determined the timings of individual extrema using the asymptotic parabola fit (Marsakova & Andronov 1996). For the analysis, we have computed sets of *simultaneous* V and R observations using the MCV software (Andronov & Baklanov 2004). This program realizes an algorithm of the local cubic interpolation of brightness in one color (e.g. V) at the times of observations in another color (e.g. R) using the sequence of VRVRVR... observations

Table 4. Characteristics of spin maxima of RXJ0625 in V and R bands obtained using the asymptotic parabola fits (Marsakova & Andronov 1996).

V			R		
$t_{max}-2453000, \sigma_t$	m_{max}, σ_m	ϕ_{max}	$t_{max}-2453000, \sigma_t$	m_{max}, σ_m	ϕ_{max}
53049.23487 0.00003	14.667 0.014	26694.7280	53049.23546 0.00017	14.278 0.042	26694.7716
53050.94289 0.00009	14.862 0.007	26819.0279	53050.94312 0.00023	14.459 0.018	26819.0448
53051.01210 0.00017	14.731 0.013	26824.0645	53051.01191 0.00009	14.323 0.006	26824.0505
53051.06852 0.00041	14.804 0.033	26828.1702	53051.06804 0.00097	14.417 0.029	26828.1351
53051.07987 0.00009	14.611 0.019	26828.9962	53051.07987 0.00015	14.232 0.028	26828.9962
53051.09538 0.00008	14.483 0.010	26830.1250	53051.09567 0.00015	14.132 0.013	26830.1464
53051.12237 0.00009	14.616 0.008	26832.0890	53051.12253 0.00008	14.245 0.009	26832.1011
53051.13595 0.00021	14.680 0.005	26833.0777	53051.13579 0.00058	14.257 0.014	26833.0656
53051.17750 0.00046	14.597 0.019	26836.1013	53051.17666 0.00002	14.242 0.011	26836.0403
53051.19187 0.00019	14.537 0.019	26837.1468	53051.19114 0.00020	14.162 0.056	26837.0937
53051.21983 0.00007	14.698 0.007	26839.1819	53051.21950 0.00011	14.274 0.006	26839.1576
53051.23170 0.00015	14.626 0.008	26840.0456	53051.23298 0.00033	14.202 0.016	26840.1388
53051.27087 0.00013	14.611 0.006	26842.8964	53051.27220 0.00022	14.177 0.011	26842.9933
53051.28552 0.00000	14.507 0.004	26843.9621	53051.28486 0.00007	14.086 0.007	26843.9140
53051.29889 0.00014	14.506 0.012	26844.9349	53051.29913 0.00016	14.125 0.020	26844.9530
53051.31415 0.00009	14.689 0.009	26846.0458	53051.31389 0.00044	14.300 0.029	26846.0268
53053.18030 0.00036	14.561 0.006	26981.8531	53053.18082 0.00047	14.163 0.020	26981.8909
53053.19555 0.00019	14.632 0.007	26982.9625	53053.19550 0.00042	14.186 0.010	26982.9592
53053.20966 0.00018	14.528 0.023	26983.9896	53053.20983 0.00026	14.105 0.048	26984.0021
53053.22247 0.00012	14.619 0.017	26984.9222	53053.22289 0.00022	14.145 0.019	26984.9526
53053.23722 0.00031	14.591 0.098	26985.9953	53053.23709 0.00039	14.161 0.021	26985.9859
53053.25023 0.00017	14.468 0.018	26986.9423	53053.25005 0.00001	14.061 0.007	26986.9293
53054.15777 0.00005	14.515 0.004	27052.9877	53054.15523 0.00018	14.090 0.006	27052.8028
53384.19294 0.00008	15.409 0.014	51070.9725	53384.19332 0.00044	14.865 0.027	51071.0001
53384.22240 0.00046	15.536 0.068	51073.1164	53384.22287 0.00056	14.977 0.088	51073.1504
53384.23666 0.00017	15.619 0.051	51074.1542	53384.23629 0.00028	15.098 0.024	51074.1269
53384.25021 0.00011	15.624 0.010	51075.1404	53384.25029 0.00043	15.143 0.036	51075.1463
53384.26495 0.00040	15.564 0.054	51076.2126	53384.26408 0.00033	15.059 0.059	51076.1494
53384.29271 0.00007	15.645 0.009	51078.2331	53384.29088 0.00000	15.184 0.008	51078.0997
53384.32682 0.00012	15.337 0.009	51080.7152	53384.32863 0.00040	14.873 0.023	51080.8472
53384.34245 0.00016	15.384 0.020	51081.8530	53384.34208 0.00021	14.755 0.013	51081.8262
53384.35446 0.00010	15.315 0.009	51082.7268	53384.35551 0.00024	14.819 0.027	51082.8034
53384.38537 0.00018	15.423 0.024	51084.9766	53384.38505 0.00041	14.912 0.039	51084.9528
53405.98375 0.00065	15.597 0.063	52656.7770	53405.98228 0.00036	15.046 0.011	52656.6701
53405.99945 0.00015	15.079 0.032	52657.9201	53405.99841 0.00028	14.782 0.020	52657.8438
53406.02728 0.00032	15.558 0.075	52659.9449	53406.02889 0.00038	15.009 0.042	52660.0623
53406.04059 0.00029	15.569 0.066	52660.9138	53406.04085 0.00027	15.092 0.038	52660.9328
53406.08265 0.00002	15.727 0.027	52663.9742	53406.08397 0.00047	15.260 0.021	52664.0707
53406.10315 0.00013	15.616 0.015	52665.4666	53406.10330 0.00056	15.219 0.030	52665.4771
53406.11543 0.00083	15.568 0.137	52666.3599	53406.11142 0.00020	15.091 0.005	52666.0685

with periodically changing filter. In the case of gaps caused by bad observations, the interpolation is not applied, and the corresponding point is removed from the resulting data set. Altogether, a set of 1009 *simultaneous* points obtained during 6 nights, have been analyzed, and 174 extrema timings have been determined.

They are listed in Tables 4 and 5 for maxima and minima, respectively. The phases of these extrema show a very large scatter, which significantly exceeds the error estimates. As a reference ephemeris, we have used that by Staude et al. (2003). The *phase−phase* diagrams have been plotted for both colors separately for the minima and maxima (Figure 5). They show a strong concentration to the line of equivalence, which indicates, that the changes of the shape in two filters are highly

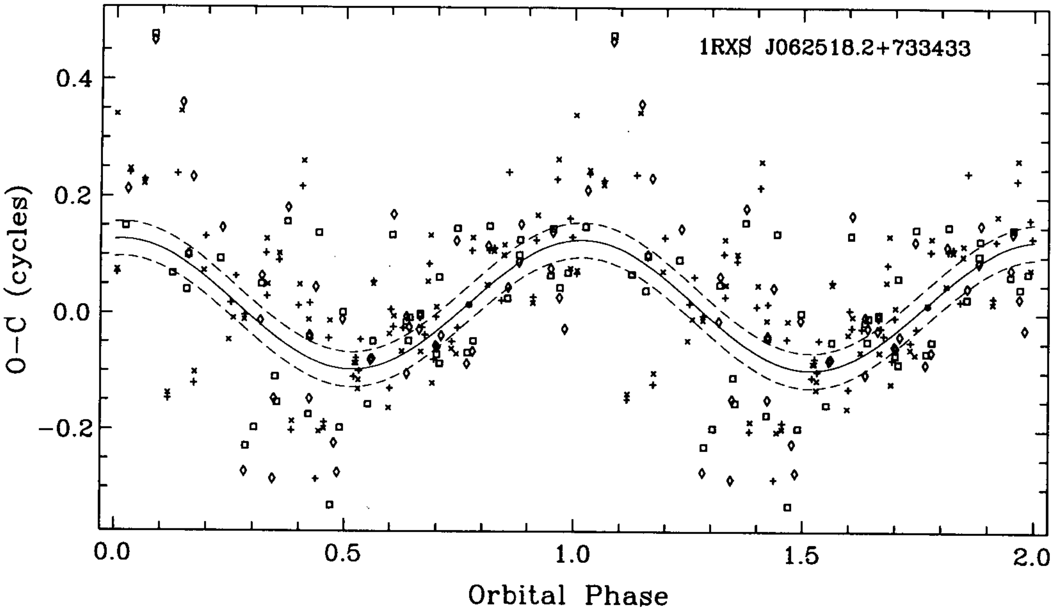

Figure 6. The phases of spin maxima (square) and minima (cross) for V (rotated by 45°) and R (not rotated) observations, as the function of the orbital phase computed according to the ephemeris by Staude et al. (2003). The solid and dashed lines correspond to the best sine fit and $\pm 1\sigma$ corridor, respectively.

correlated.

Such variability may be caused by either by the inhomegeneous accretion flow from the secondary onto the white dwarf, by periodically changing conditions of accretion because of the rotation of the white dwarf, or by periodically changing viewing conditions. To check the last suggestion, we had plotted the *spin* phase of extrema vs the the *orbital* phase using the ephemerids Eq. 6, Eq. 7 and Eq. 8. The phases of minima have been shifted by 0.5 for compatibility with the maxima.

The corresponding plot (Figure 6) for the best ephemeris (Eq. 7) shows a possible wave with a semi-amplitude of 0.11 (3) with an unsignificant period-average value of 0.015 (22). The maximum occurs at the orbital phase 0.016 (8), so practically coinciding with the orbital minimum. One may note, that the signal-to-noise ratio is the best for the ephemeris (Eq. 7) as compared with Eq. 6 and Eq. 8. The false alarm probability (FAP) to get such a wave owing to statistical fluctuations is 0.019, so the detected phenomenon seems to be statistically significant.

The profile of the spin pulses have been modeled by some authors (cf. Kim & Beuermann 1995, 1996). However, the periodic changes with the orbital phase are the observational fact, which is to be interpreted in future theoretic models.

8. CONCLUSIONS

The analysis of two-color VR photometry obtained at the telescopes of the Korea Astronomy and Space Science Institute in 2004-2005, had lead to the corrected spin and orbital period. We could present some new results of the time series analysis. Other results can be summarised as following:

Table 5. Characteristics of spin minima of RXJ0625 in V and R bands obtained using the asymptotic parabola fits (Marsakova & Andronov 1996).

t_{min} − 2453000, σ_t	m_{min}, σ_m	ϕ_{min}	t_{min} − 2453000, σ_t	m_{min}, σ_m	ϕ_{min}
53049.17784 0.00040	14.895 0.010	26690.5780	53049.17858 0.00196	14.479 0.006	26690.6315
53049.20236 0.00024	14.952 0.011	26692.3624	53049.20223 0.00022	14.550 0.009	26692.3528
53050.95041 0.00018	15.083 0.034	26819.5750	53050.95033 0.00018	14.644 0.010	26819.5693
53051.01950 0.00010	15.049 0.023	26824.6026	53051.01934 0.00012	14.586 0.014	26824.5913
53051.06001 0.00002	15.092 0.017	26827.5510	53051.06007 0.00064	14.613 0.038	26827.5553
53051.07215 0.00030	15.007 0.039	26828.4346	53051.07270 0.00016	14.608 0.018	26828.4747
53051.08695 0.00026	14.946 0.045	26829.5118	53051.08671 0.00032	14.502 0.067	26829.4940
53051.10233 0.00014	14.833 0.009	26830.6306	53051.10201 0.00040	14.404 0.017	26830.6078
53051.11590 0.00016	14.863 0.011	26831.6181	53051.11761 0.00019	14.491 0.014	26831.7426
53051.12827 0.00018	14.949 0.009	26832.5188	53051.12842 0.00027	14.539 0.014	26832.5292
53051.14643 0.00014	14.868 0.010	26833.8402	53051.14401 0.00036	14.415 0.010	26833.6638
53051.18398 0.00000	14.861 0.007	26836.5732	53051.18478 0.00032	14.432 0.030	26836.6314
53051.19660 0.00012	14.777 0.009	26837.4915	53051.19760 0.00025	14.346 0.007	26837.5637
53051.21115 0.00010	14.926 0.011	26838.5502	53051.21087 0.00000	14.493 0.005	26838.5295
53051.22488 0.00001	14.870 0.016	26839.5495	53051.22439 0.00002	14.392 0.013	26839.5135
53051.23777 0.00024	14.790 0.006	26840.4875	53051.23736 0.00105	14.347 0.015	26840.4572
53051.25011 0.00051	14.807 0.039	26841.3857	53051.25107 0.00059	14.392 0.026	26841.4550
53051.26537 0.00020	14.949 0.015	26842.4960	53051.26511 0.00022	14.500 0.018	26842.4770
53051.28102 0.00000	14.814 0.006	26843.6346	53051.28035 0.00048	14.375 0.029	26843.5857
53051.29195 0.00019	14.818 0.016	26844.4306	53051.29257 0.00017	14.385 0.027	26844.4755
53051.30812 0.00013	14.923 0.009	26845.6071	53051.30819 0.00013	14.483 0.008	26845.6123
53053.14656 0.00004	14.872 0.004	26979.3980	53053.14630 0.00024	14.439 0.018	26979.3791
53053.16108 0.00010	14.869 0.009	26980.4541	53053.16195 0.00030	14.418 0.017	26980.5177
53053.17721 0.00041	14.828 0.031	26981.6280	53053.17687 0.00091	14.407 0.044	26981.6035
53053.19278 0.00034	14.804 0.020	26982.7613	53053.19218 0.00263	14.360 0.036	26982.7177
53053.21550 0.00019	14.833 0.017	26984.4148	53053.21562 0.00037	14.364 0.026	26984.4237
53053.22993 0.00011	14.831 0.010	26985.4650	53053.23051 0.00007	14.373 0.005	26985.5074
53053.24325 0.00071	14.742 0.124	26986.4345	53053.24383 0.00027	14.334 0.014	26986.4762
53054.15092 0.00022	14.768 0.017	27052.4892	53054.15103 0.00057	14.327 0.040	27052.4970
53054.17840 0.00007	14.881 0.032	27054.4888	53054.17880 0.00004	14.408 0.004	27054.5178
53384.19855 0.00031	15.921 0.013	51071.3805	53384.19910 0.00002	15.341 0.002	51071.4211
53384.21415 0.00035	15.951 0.008	51072.5158	53384.21414 0.00101	15.363 0.009	51072.5154
53384.22906 0.00011	15.940 0.013	51073.6007	53384.22798 0.00027	15.456 0.019	51073.5227
53384.24374 0.00020	15.900 0.016	51074.6692	53384.24314 0.00026	15.394 0.034	51074.6260
53384.27194 0.00085	15.861 0.036	51076.7216	53384.27204 0.00114	15.349 0.006	51076.7290
53384.28738 0.00047	16.021 0.038	51077.8450	53384.28592 0.00079	15.378 0.038	51077.7386
53384.33505 0.00033	15.662 0.052	51081.3143	53384.33483 0.00017	15.060 0.013	51081.2982
53384.34862 0.00014	15.667 0.024	51082.3021	53384.34877 0.00007	15.079 0.007	51082.3129
53384.36330 0.00002	15.885 0.003	51083.3700	53384.36372 0.00002	15.328 0.023	51083.4006
53384.37659 0.00013	15.886 0.015	51084.3376	53384.37705 0.00001	15.324 0.019	51084.3712
53384.39332 0.00022	16.009 0.037	51085.5552	53384.39206 0.00035	15.329 0.030	51085.4634
53405.97715 0.00002	15.849 0.007	52656.2968	53405.97602 0.00010	15.254 0.020	52656.2149
53405.99251 0.00100	15.795 0.041	52657.4146	53405.99218 0.00066	15.227 0.040	52657.3906
53406.03407 0.00008	15.980 0.025	52660.4395	53406.03424 0.00025	15.462 0.034	52660.4519
53406.04933 0.00007	16.500 0.009	52661.5497	53406.05014 0.00016	15.876 0.057	52661.6085
53406.07977 0.00001	15.961 0.026	52663.7646	53406.07930 0.00018	15.493 0.021	52663.7305
53406.09326 0.00052	16.100 0.030	52664.7465	53406.09317 0.00048	15.611 0.021	52664.7401

- The periodic modulation of the spin phases with an orbital phase has been found. It should be checked by further monitoring of this interesting object, as well by an analysis of other intermediate polars.

- The periodic phase shift may affect also the nightly-mean phases, thus it is recommended to try to observe at least during a complete orbital period (5^h).

- The periodicity of seasons of observations (nearly at the same month) causes serious problems with cycle numbering of such short-periodic objects. Thus a further monitoring should be carried out, being distributed over the season of the visibility of the object.

ACKNOWLEDGEMENTS: This work was supported by the research grant of the Chungbuk National University in 2005 and partially supported by the Ministry of Education and Science of Ukraine.

REFERENCES

Andronov, I. L. 1991, Kinem. Phys. Celest. Bodies, 7, 78

Andronov, I. L. 1994, Odessa Astronomical Publications, 7, 49

Andronov, I. L. 1997, A&AS 125, 207

Andronov, I. L. 2001, Odessa Astronomical Publications, 14, 255

Andronov, I. L., Antoniuk, K. A., Augusto, P., Baklanov, A. V., Chinarova, L. L., Chochol, D., Efimov, Yu. S., Gazeas, K., Halevin, A. V., Kim, Y., Kolesnikov, S. V., Kudashkina, L. S., Marsakova, V. I., Mason, P. A., Niarchos, P. G., Nogami, D., Ostrova, N. I., Patkos, L., Pavlenko, E. P., Shakhovskoy, N. M., Tremko, J., Yushchenko, A. V., & Zola, S. 2003, Astronomy and Astrophysics Transcactions, 22, 793

Andronov, I. L., & Baklanov, A. V. 2004, Astronical School Reports, 5, 264

Andronov, I. L., Kim, Y., & Kolesnikov, S. V. 2005a, in preparation

Andronov, I. L., Kim, Y., Shin J.-H., & Jeon, Y. B. 2005b, Astronomical Society of Pacific Conference Series, 335, 355

Andronov, I. L., Ostrova, N. I., & Burwitz, V. 2005c, Astronomical Society of Pacific Conference Series, 335, 229

Araujo-Betancor, S., Gänsicke, B. T., Hagen, H.-J., Rodriguez-Gil, P., & Engels, D. 2003, A&A, 406, 213

Gliese, W., & Fahress, H. 1979, A&AS, 38, 423

Hellier, C. 2001, Cataclysmic Variable Stars. How and why they vary (Berlin: Springer Verlag)

Henden, A. 2004a, ftp://ftp.nofs.navy.mil/pub/outgoing/aah/sequence/j0625.dat

Henden, A. 2004b, ftp://ftp.nofs.navy.mil/pub/outgoing/aah/sequence/v1315aql.dat

Kim, Y., Andronov, I. L., Park, S. S., & Jeon, Y.-B. 2005a, A&A (accepted), Astro/ph 0507086

Kim, Y., Andronov, I. L., Park, S. S., & Kim, C.-H. 2005b, The Astronomer, 41, 323

Kim, Y., Andronov, I. L., Park, S. S., & Kim, C.-H. 2005c, Information Bulletin On Variable Stars, 5700

Kim, Y. G., Andronov, I. L., & Jeon, Y. B. 2004, JA&SS, 21, 191

Kim, Y., & Beuermann, K. 1995, A&A 298, 165

Kim, Y., & Beuermann, K. 1996, A&A 307, 824

Marsakova, V. I., & Andronov, I. L. 1996, Odessa Astronomical Publications, 9, 127

Massey, P., & Davis, L. E. 1992, A User's Guide to Stellar CCD photometry with IRAF

Patterson, J. 1994, PASP, 106, 209

Staude, A., Schwope, A. D., Krumpe, M., Hambaryan, V., & Schwarz, R. 2003, A&A, 406, 253

Warner, B. 1986, MNRAS, 219, 347

Warner, B. 1995, Cataclysmic Variable Stars (Cambridge: Cambridge Univ. Press)

Wei, J. Y., Xu, D. W., Dong, X. Y., & Hu, J. Y. 1999, A&AS, 139, 575